J. Am. Chem. Soc. **1992**, *114*, 6621–6630

Bicyclo[2.2.2]octane-Capped Porphyrins. 1. Synthesis, Characterization, and Solution Three-Dimensional Structure

Hong-Yue Zhang, Andrei Blaskó, Jian-Qiu Yu, and Thomas C. Bruice*

Contribution from the Department of Chemistry, University of California at Santa Barbara, Santa Barbara, California 93106.
Received February 24, 1992

Abstract: Three novel capped porphyrins {bicyclo[2.2.2]octane-capped porphyrins, **VIAH$_2$** and **VIBH$_2$**, and bicyclo[2.2.2]-oct-7-ene-capped porphyrin, **VICH$_2$**} have been successfully synthesized by the Lewis acid ($BF_3{\cdot}Et_2O$) catalyzed condensation of pyrrole with tetraacetals **6**, **12**, and **15**, respectively. ^{1}H and ^{13}C 1D and ^{1}H–^{1}H 2D NMR (DQF-COSY and ROESY) of porphyrins **VIAH$_2$** and **VIBH$_2$** and ^{1}H 1D and 2D NMR of **VICH$_2$** established that the bridges of the bicyclo[2.2.2]octane-caps are pointing outside the cavity formed between the cap and the porphyrin plane. The three-dimensional structure of **VIAH$_2$** in solution has been determined using ROESY and Distance Geometry calculations, and the size of the cavity formed between porphyrin and cap has been shown to be only large enough to accommodate a single H_2O. The corresponding iron(III) complexes of **VIAH$_2$** {(VIA)Fe^{III}(X) where X = Cl$^-$ or SbF$_6^-$} have been prepared and characterized. Equilibrium binding experiments of *N*-methylimidazole to (VIA)Fe^{III}(SbF$_6$) show that only one nitrogen base can be ligated.

Introduction

An impetus to the design and synthesis of superstructural porphyrins[1] has been the desire to obtain mimics of the catalytic properties of heme-containing enzymes. For example, capped, bridged, and strapped porphyrins have been designed as models to mimic the oxygen binding to hemoglobin and myoglobin,[2] the reduction of dioxygen by cytochrome C oxidase,[3] the oxidations catalyzed by cytochrome P-450 enzymes,[4] and the electron transfer processes at photosynthetic reaction centers.[5]

Of continuing interest in this laboratory[6] is the challenge to synthesize quadruply capped tetraphenylporphyrins to be employed in the design of catalysts. Baldwin was the first to synthesize capped porphyrins (**IH$_2$** and **IIH$_2$**).[7] Porphyrins **IH$_2$** and **IIH$_2$** are capped by a phenyl ring attached to four ester linkers which are in turn covalently connected to a tetraphenylporphyrin by ether linkages. Recently, Ibers reported the synthesis of two capped porphyrins (**IIIH$_2$** and **IVH$_2$**)[8] similar to **IH$_2$** and **IIH$_2$** using ether and amide linkages. Tetraphenylporphyrins whose *meso*-phenyl moieties are substituted in the ortho positions by alkoxy substituents are quite susceptible to destructive oxidation[9] and ester linkages are susceptible to hydrolysis. The structures **IH$_2$**, **IIH$_2$**, **IIIH$_2$**, and **IVH$_2$** are, therefore, susceptible to destructive oxidation and hydrolysis.[6b]

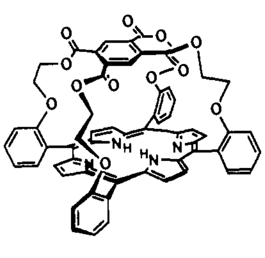

IH_2

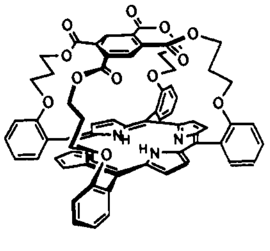

IIH_2

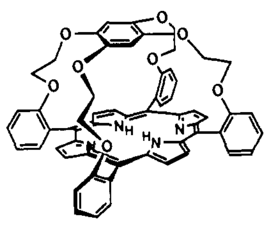

$IIIH_2$

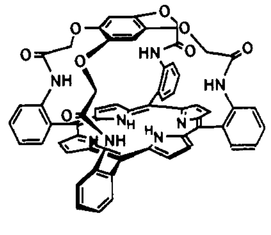

IVH_2

In the design of complex catalysts we have a need for new capping structures which must be resistant to oxidation and hydrolysis and which restrict approach of reagents to the distal side of the porphyrin ring. Recently, we reported the synthesis of **VH$_2$** which has a completely hydrocarbon cap[6b] ($C_{70}H_{68}N_4$). In the structure of **VH$_2$** a phenyl ring acts as a "keystone" for attachment of four pentamethylene arches which are attached to tetraphenylporphyrin phenyl substituents. Unfortunately, the synthesis of this capped porphyrin involves many steps and the overall yield is low, thus restricting its applications to future uses. We now report the design and synthesis of a series of three capped porphyrins (**VIAH$_2$**, **VIBH$_2$**, and **VICH$_2$**, Chart I) based on a bicyclo[2.2.2]octane "keystone". Much like **VH$_2$**, structures **VIAH$_2$**, **VIBH$_2$**, and **VICH$_2$** are characterized by the attachment of the capping structure to tetraphenylporphyrin moiety via a C–C bond. We have used ^{1}H NMR (DQF-COSY, ROESY) combined with Distance Geometry calculations to define the structure of **VIAH$_2$** and its cavity formed between the porphyrin ring and the cap in $CDCl_3$ solution.

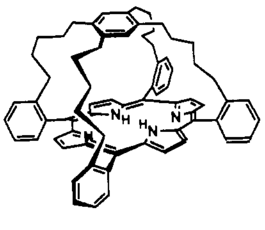

VH_2

---

(1) (a) Morgan, B.; Dolphin, D. *Struct. Bonding (Berlin)* **1987**, *64*, 115. (b) Baldwin, J. E.; Perlmutter, P. *Top. Curr. Chem.* **1984**, *121*, 181.

(2) (a) Traylor, T. G. *Acc. Chem. Res.* **1981**, *14*, 102. (b) Momenteau, M. *Pure Appl. Chem.* **1986**, *58*, 1493.

(3) Collman, J. P.; Anson, F. C.; Barnes, C. E.; Bencosme, C. S.; Geiger, T.; Evitt, E. R.; Kreh, R. P.; Meier, K.; Pettman, R. B. *J. Am. Chem. Soc.* **1983**, *105*, 2694.

(4) (a) Collman, J. P.; Brauman, J. I.; Fitzgerald, J. P.; Hampton, P. D.; Naruta, Y.; Michida, T. *Bull. Chem. Soc. Jpn.* **1988**, *61*, 47. (b) Groves, J. T.; Viski, P. *J. Org. Chem.* **1990**, *55*, 3628.

(5) (a) Krieger, C.; Weiser, J.; Staab, H. A. *Tetrahedron Lett.* **1985**, *26*, 6055. (b) Lindsey, J. S.; Delaney, J. K.; Mauzerall, D. C.; Linschitz, H. *J. Am. Chem. Soc.* **1988**, *110*, 3610. (c) Mauzerall, D.; Weiser, J.; Staab, H. *Tetrahedron* **1989**, *45*, 4807.

(6) (a) Lee, C. H.; Garcia, B.; Bruice, T. C. *J. Am. Chem. Soc.* **1990**, *112*, 6434. (b) Schnatter, W. F. K.; Almarsson, O.; Bruice, T. C. *Tetrahedron* **1991**, *47*, 8687. (c) Garcia, B.; Lee, C. H.; Blasko, A.; Bruice, T. C. *J. Am. Chem. Soc.* **1991**, *113*, 8118.

(7) (a) Almog, J.; Baldwin, J. E.; Crossley, M. J.; Debernardis, J. F.; Dyer, R. L.; Huff, J. R.; Peters, M. K. *Tetrahedron* **1981**, *37*, 3589. (b) Almog, J.; Baldwin, J. E.; Dyer, R. L.; Peter, M. *J. Am. Chem. Soc.* **1975**, *97*, 226.

(8) Johnson, M. R.; Seok, W. K.; Ibers, J. A. *J. Am. Chem. Soc.* **1991**, *113*, 3998.

(9) (5,10,15,20-Tetrakis(*p*-methoxyphenyl)porphyrinato)iron(III) is destructively oxidized by weak oxidants such as *p*-cyano-*N*,*N*-dimethylaniline *N*-oxide. Lee, R. W.; Bruice, T. C. Unpublished results.

0002-7863/92/1514-6621$03.00/0

Chart I

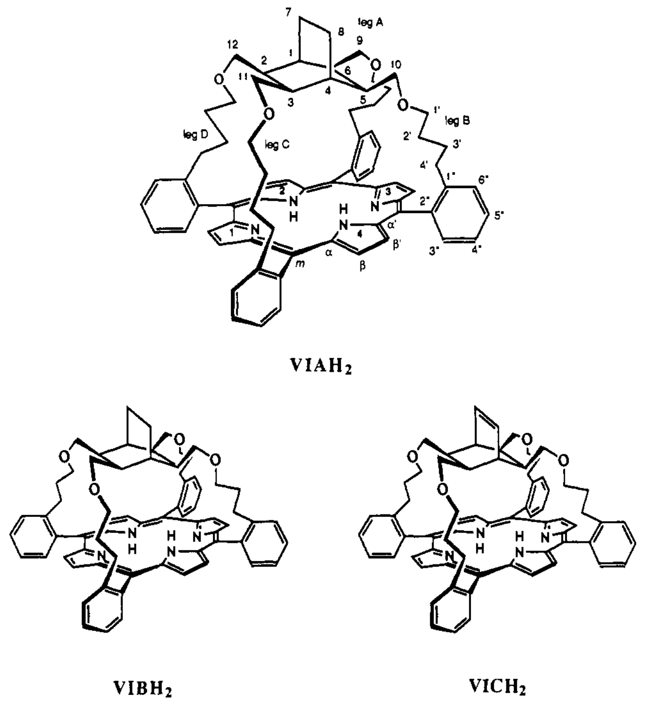

VIAH$_2$

VIBH$_2$ VICH$_2$

Results and Discussion

There are various methods by which a tetraphenylporphyrin ring can be constructed.[10] One procedure is to react pyrrole with an appropriate benzaldehyde.[7,11-13] Baldwin and co-workers,[7] in the synthesis of **IH$_2$** and **IIH$_2$**, introduced the idea of incorporating four benzaldehyde moieties into a single structure which reacted with pyrrole to afford the desired capped tetraphenylporphyrin (Scheme I). We have employed this strategy in the synthesis of **VIAH$_2$**, **VIBH$_2$**, and **VICH$_2$** using Lewis acid catalyzed condensation of aldehyde and pyrrole moieties (Lindsey's method[13]).

Synthesis of Capped Porphyrins: (a) VIAH$_2$. 2-*syn*,3-*syn*,5-*syn*,6-*syn*-Tetrakis(hydroxymethyl)bicyclo[2.2.2]octane (**3**)[14] was obtained in 75% yield from hydrogenation of tetraethyl bicyclo[2.2.2]oct-7-ene-2-*syn*,3-*syn*,5-*syn*,6-*syn*-tetracarboxylate (**1**)[15] followed by reduction of the resultant tetraethyl bicyclo[2.2.2]octane-2-*syn*,3-*syn*,5-*syn*,6-*syn*-tetracarboxylate (**2**) as shown in Scheme II. 2-[2′-(4″-Bromobutyl)phenyl]-1,3-dioxolane (**5**) was prepared in high yield from the reaction of 2-(2′-bromophenyl)-1,3-dioxolane (**4**)[16] with magnesium followed by treatment with an excess of 1,4-dibromobutane in the presence of cuprous bromide in HMPA–THF[17] (Scheme III).

The coupling reaction of **3** with **5** in the presence of sodium hydride in HMPA gave only 7% of 2-*syn*,3-*syn*,5-*syn*,6-*syn*-tetrakis{4′-[2″-(1‴,3‴-dioxolan-2‴-yl)phenyl]butoxymethyl}bicyclo[2.2.2]octane (**6**). When potassium hydride was used as a base, **6** was obtained in 67% yield. Deprotection of **6** in wet acetone catalyzed by pyridinium *p*-tosylate gave 2-*syn*,3-*syn*,5-*syn*,6-*syn*-tetrakis{4′-[2″-formylphenyl]butoxymethyl}bicyclo[2.2.2]octane (**7**) in 85% yield (Scheme IV).

Scheme I

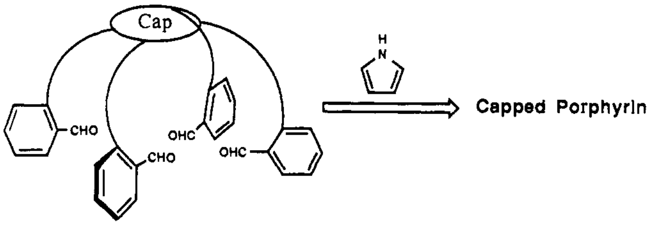

Scheme II

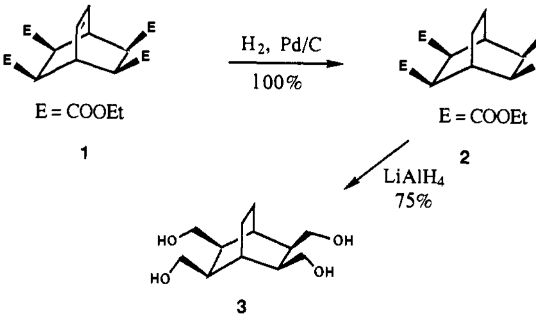

1 2 3

Scheme III

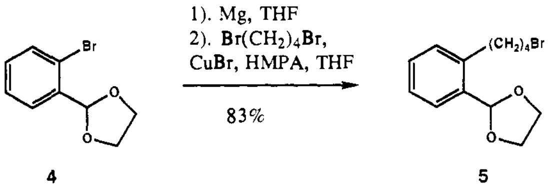

4 5

By using Baldwin's method,[7] treatment of **7** with pyrrole in dry refluxing propanoic acid afforded **VIAH$_2$** in 4% yield. When Lindsey's method[13] was used, **VIAH$_2$** was obtained in 6% yield from a high dilution coupling of **7** with pyrrole in the presence of boron trifluoride etherate followed by 2,3-dicyano-5,6-dichloroquinone (DDQ) oxidation of the resultant porphyrinogen.

Because acidic conditions are generally employed in the synthesis of porphyrinogen rings, it occurred to us that a shortcut could be taken such that hydrolysis of **6** to **7** could be combined with the condensation of the aldehyde with pyrrole. Treatment of **6** with pyrrole and boron trifluoride etherate in chloroform at high dilution ($\sim 10^{-3}$ M) followed by oxidation of porphyrinogen with DDQ gave **VIAH$_2$** in 11% yield (Scheme IV). Use of boron trichloride in place of boron trifluoride etherate afforded **VIAH$_2$** in the same yield.

(b) VIBH$_2$. Ozonolysis of 3-methoxy-1,2-dihydronaphthalene (**8**)[18] in dichloromethane (–78 °C) in the presence of Sudan red 7B as an indicator followed by protection of the aldehyde functional group with ethylene glycol catalyzed by pyridinium *p*-tosylate provided 2-[2′-(3″-oxy-3″-methoxy)propyl]phenyl-1,3-dioxolane (**9**) in 68% yield. Reduction of **9** by lithium aluminum hydride in THF afforded the corresponding alcohol 2-[2′-(3″-hydroxypropyl)phenyl-1,3-dioxolane (**10**) which was reacted with mesyl chloride in pyridine and then treated with tetra-*n*-butylammonium bromide in acetone to give 2-[2′-(3″-bromopropyl)]phenyl-1,3-dioxolane (**11**) in 93% yield (Scheme V).

Condensation of **3** with **11** in the presence of potassium hydride in HMPA afforded 2-*syn*,3-*syn*,5-*syn*,6-*syn*-tetrakis{3′-[2″-(1‴,3‴-dioxolan-2‴-yl)phenyl]propoxymethyl}bicyclo[2.2.2]octane (**12**) in 77% yield. Deprotection of **12** catalyzed by pyridinium *p*-tosylate in wet acetone gave 2-*syn*,3-*syn*,5-*syn*,6-*syn*-tetrakis{3′-[2″-formylphenyl]propoxymethyl}bicyclo[2.2.2]octane (**13**) in 87% yield. The capped porphyrin **VIBH$_2$** was obtained from both **12** and **13**, in 4% and 2% yields, respectively (Scheme IV). The lower yield of **VIBH$_2$** when compared to **VIAH$_2$** is attributed to the greater steric hindrance in the formation of the former.

---

(10) Smith, K. M. Synthesis and Preparation of Porphyrin Compounds. In *Porphyrins and Metalloporphyrins*; Smith, K. M., Ed.; Elsevier Scientific Publishing Co.: New York; 1975, p 32.

(11) Rothemund, L. *J. Am. Chem. Soc.* **1936**, *58*, 625.

(12) Adler, A. D.; Longo, F. R.; Finarelli, J. D.; Goldmacher, J.; Assour, J.; Korsakoff, L. *J. Org. Chem.* **1967**, *32*, 476.

(13) (a) Lindsey, J. S.; Schreiman, I. C.; Hsu, H. C.; Kearney, P. C.; Marguerettaz, A. M. *J. Org. Chem.* **1987**, *52*, 827. (b) Wagner, R. W.; Lawrence, D. S.; Lindsey, J. S. *Tetrahedron Lett.* **1987**, *28*, 3069. (c) Lindsey, J. S.; Wagner, R. W. *J. Org. Chem.* **1989**, *54*, 828.

(14) Chollet, A.; Wismer, M.; Vogel, P. *Tetrahedron Lett.* **1976**, 4271.

(15) Gabioud, R.; Vogel, P. *Tetrahedron* **1980**, *36*, 149.

(16) Wytko, J. A.; Weiss, J. *J. Org. Chem.* **1990**, *55*, 5200.

(17) Nishimura, J.; Yamada, N.; Horiuchi, Y.; Ueda, E.; Ohbayashi, A.; Oku, A. *Bull. Chem. Soc. Jpn.* **1986**, *59*, 2035.

(18) Taskinen, E.; Kuusisto, M. *Acta Chem. Scand. Ser B* **1985**, *B39*, 495.

Scheme IV

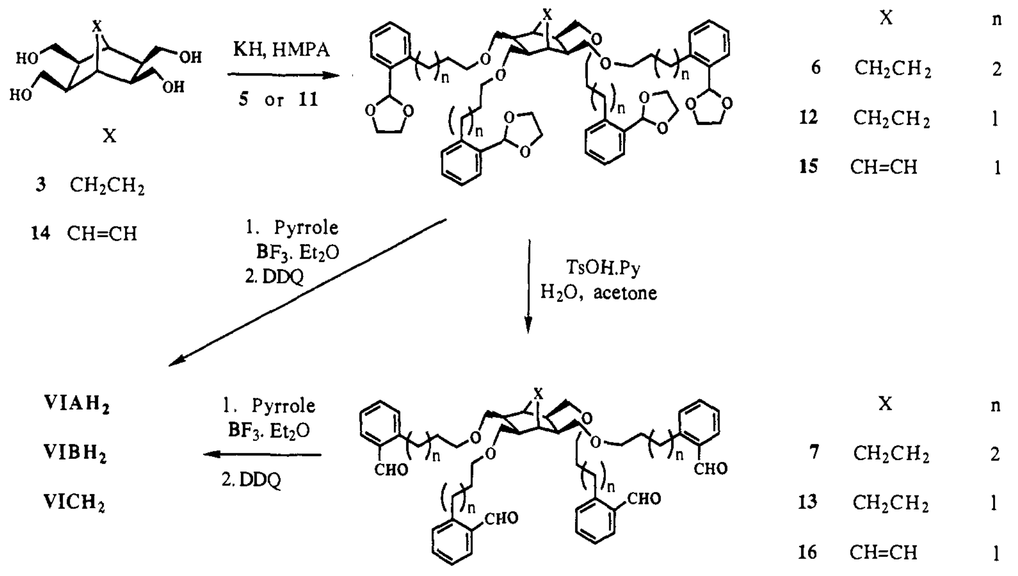

Scheme V

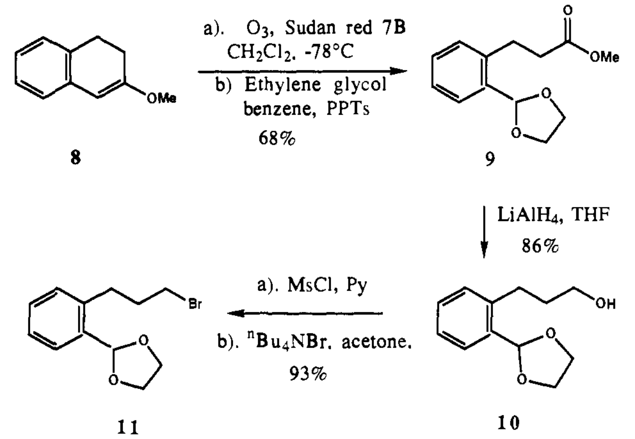

(c) **VICH$_2$.** By using the same procedures as in Scheme IV, condensation of 2-*syn*,3-*syn*,5-*syn*,6-*syn*-tetrakis(hydroxymethyl)bicyclo[2.2.2]oct-7-ene (**14**)[19] with **11** in the presence of potassium hydride in HMPA afforded 2-*syn*,3-*syn*,5-*syn*,6-*syn*-tetrakis{3′-[2″-(1‴,3‴-dioxolan-2‴-yl)phenyl]propoxymethyl}-bicyclo[2.2.2]oct-7-ene (**15**) in 89% yield. Deprotection of **15** gave 2-*syn*,3-*syn*,5-*syn*,6-*syn*-tetrakis{3′-[2″-formylphenyl]propoxymethyl}bicyclo[2.2.2]oct-7-ene (**16**) in 88% yield. Coupling of **15** and **16** with pyrrole followed by DDQ oxidation of the resultant porphyrinogens gave **VICH$_2$** in 4% and 2% yields, respectively (Scheme IV).

Characterization of Capped Porphyrins. The capped porphyrins **VIAH$_2$**, **VIBH$_2$**, and **VICH$_2$** were characterized by low- and high-resolution FABMS, ^{1}H NMR, ^{13}C NMR, ^{1}H–^{1}H 2D NMR (DQF-COSY and ROESY), IR, and UV/vis spectroscopies. Low-resolution FABMS of **VIAH$_2$** gave a molecular weight of 1060 which is that expected of the formula of **VIAH$_2$** ($C_{72}H_{76}N_4O_4$). High-resolution FABMS of **VIAH$_2$** gave an exact mass of 1061.5946 which corresponds to the formula of $C_{72}H_{77}N_4O_4$ [$(M + H)^+$, calcd 1061.5945]. IR of **VIAH$_2$** shows an N–H absorbance at 3270 cm^{-1}. The strong Soret band at 420 nm and α,β bands at 515.5, 549, 592.5, and 646.5 nm show the presence of a porphyrin ring.

Assignments of the ^{1}H resonances of **VIAH$_2$** were based on the previous assignments of its precursors (**6** and **7** in Scheme IV) and ^{1}H–^{1}H 2D NMR (DQF-COSY and ROESY) experiments under the conditions given in the Experimental Section. In the ^{1}H NMR spectrum of **VIAH$_2$**, β-pyrrole resonances appear at 8.627 and 8.599 ppm as sharp peaks. The resonance at −2.41 ppm disappeared upon addition of a trace of D$_2$O, therefore this peak was assigned to NH protons.

The 2,3,5,6-**H** (abbreviated as 2-H; for the numbering of the protons please see Chart I, **VIAH$_2$**) resonances of **6** and **7** are broad at around 2.1 ppm and the 7,8-H (abbreviated as 7-H) resonances are sharp at around 1.4 ppm (ratio of 2-H and 7-H is 1:1). In the DQF-COSY spectrum of **6**, there is a correlation between 7-H (1.400 ppm) and 1,4-H (1.699 ppm, abbreviated as 1-H), and correlations between 2-H (2.098 ppm) and 9,11-H (3.35 ppm) as well as 10,12-H (3.55 ppm). The same types of resonances and correlations can be seen in the ^{1}H 1D and 2D NMR spectrum (Figure 1) of **VIAH$_2$**: (1) a sharp peak at 0.316 ppm couples with a peak at −0.228 ppm which was assigned as 1-H (ratio of these two peaks is 2:1); (2) a broad peak at −2.355 ppm correlates two multiplets peaks at 2.174 and 2.265 ppm which were assigned as 9a,10a,11a,12a-H (abbreviated as 9a-H) and 9b,10b,11b,12b-H (abbreviated as 9b-H). Therefore, this sharp peak is 7-H and the broad peak is 2-H.

Separate evidence for the 7-H and 2-H assignments comes from the ^{1}H NMR spectra of **VIBH$_2$** and **VICH$_2$** (Table I). In both **VICH$_2$** and **VIBH$_2$** there is a broad common resonance at around

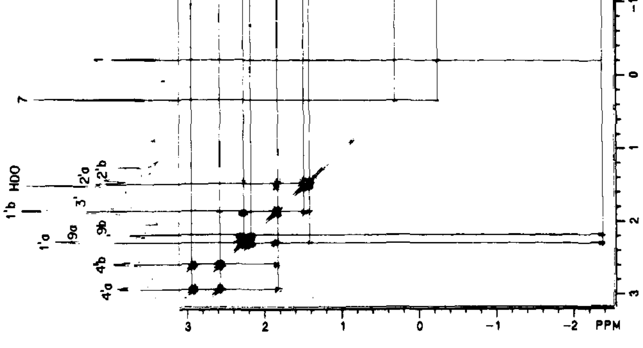

Figure 1. 500-MHz DQF-COSY spectrum of **VIAH$_2$** (partial contour plot) in CDCl$_3$ at 25 °C.

---

(19) Gabioud, R.; Vogel, P. *Helv. Chim. Acta* **1983**, *66*, 1134.

Table I. Variation of the ^{1}H Chemical Shifts from Tetraacetals to Porphyrins[a]

		δ		
		1-H	2-H	7-H
C4	**6**	1.699	2.098	1.400
	VIAH$_2$	−0.228	−2.355	0.316
	$\Delta\delta$[b]	−1.927	−4.453	−1.084
C3 sat	**12**	1.838	2.191	1.507
	VIBH$_2$	−0.321	−3.201	0.128
	$\Delta\delta$	−2.159	−5.392	−1.379
C3 unsat	**15**	2.609	2.283	6.233
	VICH$_2$	0.794	−3.195	5.032
	$\Delta\delta$	−2.112	−5.478	−1.201

[a] δ in ppm, at 25 °C, in CDCl$_3$. [b] $\Delta\delta = \delta_{porphyrin} - \delta_{acetal}$.

Table II. ^{1}H Chemical Shifts[a] for **VIAH$_2$**, **VIBH$_2$**, and **VICH$_2$**

	δ		
protons	**VIAH$_2$**	**VIBH$_2$**	**VICH$_2$**
1	−0.228 (s)	−0.321 (s)	0.794 (t, 3.5)
2	−2.355 (s)	−3.201 (s)	−3.195 (s)
7	0.316 (s)	0.128 (s)	5.032 (dd, 3.5, 4)
9a	2.265 (m)	1.918 (m)	1.522 (m)
9b	2.174[b]	1.409 (m)	1.235 (m)
1′a	2.276 (m)	3.453 (m)	3.496 (m)
1′b	1.847 (m)	2.783 (m)	2.800 (m)
2′a	1.474 (m)	1.826 (m)	1.840 (m)
2′b	1.422 (m)	1.729 (m)	1.716 (m)
3′a	1.847 (m)	2.995 (m)	3.042 (m)
3′b	1.847[c]	2.995 (m)	2.886 (m)
4′a	2.919 (m)		
4′b	2.574 (m)		
3″	7.766 (d, 7.5)	7.731 (d, 6.5)	7.740 (d, 7.5)
4″	7.419 (t, 7.5)	7.399 (t, 6.5)	7.392 (t, 7.5)
5″	7.711 (t, 7.5)	7.678 (t, 6.5)	7.678 (t, 7.5)
6″	7.747 (d, 7.5)	7.652 (d, 6.5)	7.600 (d, 7.5)
β	8.627 (s)	8.685 (s)	8.667 (s)
β′	8.599 (s)	8.574 (s)	8.578 (s)
NH	−2.41 (s)	−2.51 (s)	−2.51 (s)

[a] δ, in ppm (s, singlet, d, doublet, t, triplet, m, multiplet), at 25 °C, in CDCl$_3$. Data in parentheses are coupling constant (Hz). [b] Overlapped with 1′a. [c] Overlapped with 1′b.

−3.2 ppm and two different resonances at 5.032 (dd) and 0.128 (s) ppm. The resonance at 5.032 ppm pertains to the olefinic protons (7-H) of **VICH$_2$** and that at 0.128 ppm to the aliphatic protons 7 and 8 of **VIBH$_2$**. Therefore, the resonances at ca. −3.2 ppm is clearly that of the 2-H. The large upfield shift ($\Delta\delta$) of the 2-H resonances in **VIAH$_2$**, **VIBH$_2$**, and **VICH$_2$** (Table I) denotes that these protons must be strongly shielded. For this to occur the bridge of the cap (i.e., C7–C8) must point outwards and the 2-H downwards toward the porphyrin ring.

Once the 7-H are differentiated from the 2-H it is possible to assign the remaining resonances by DQF-COSY experiment (Table II, Figure 1). The chemical shifts of two geminal protons (a and b) on each methylene carbon are different, and the difference is greater for 1′-H ($\Delta\delta$ = 0.402 ppm) and 4′-H ($\Delta\delta$ = 0.375 ppm) than for 2′-H ($\Delta\delta$ = 0.052 ppm). This is due to the shielding effect of the porphyrin core. No effect can be seen on 3′-H, partly because of the overlapping of the 1′b-H resonance (broad signal with unresolved shoulders at 1.874 ppm), and partly because they are pointing to the outside and away from the shielding cone of the porphyrin ring. The porphyrins **VIBH$_2$** and **VICH$_2$** were characterized in the same manner as described for **VIAH$_2$** (Table II).

ROESY Calculations. The structural and conformational analysis of **VIAH$_2$** in CDCl$_3$ solution was achieved by quantifying the ROESY experimental data. To avoid the spin diffusion contribution to the ROESY peaks, the linearity of the NOE enhancements was checked for different mixing times, τ_m = 50–200 ms. The quantitative treatment of the data from τ_m = 50 ms is more difficult due to the small ROESY peaks between spins involved in the magnetization transfer, and as the distance increases they disappear in the t_1 noise. Therefore we used the data from τ_m = 200 ms in our calculations which is still in the linear part of the NOE buildup.

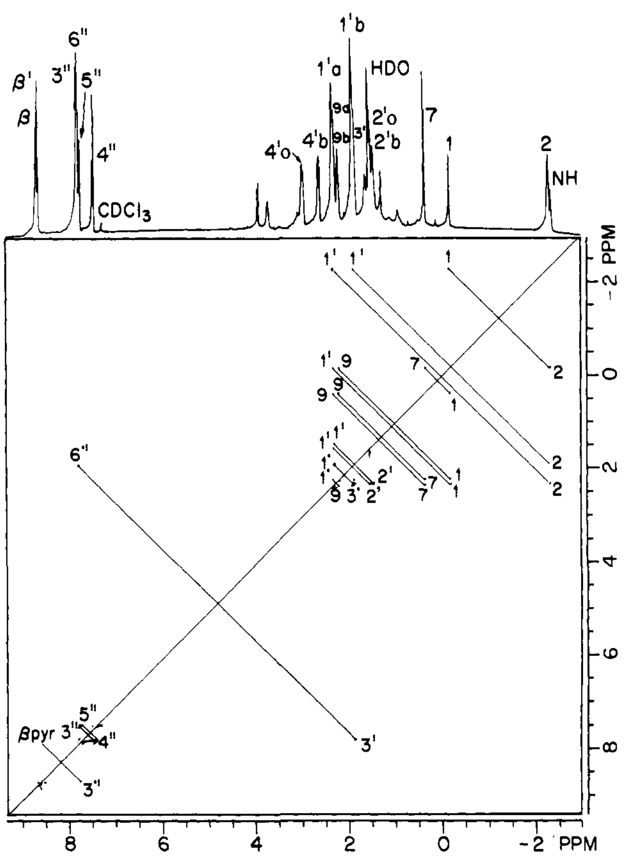

Figure 2. 500-MHz ROESY spectrum of **VIAH$_2$** in CDCl$_3$ at 25 °C with a mixing time of τ_m = 200 ms and a spin locking field strength of 4.6 kHz. The through-space interactions are shown with solid lines.

Proximities between the protons in the bicyclo[2.2.2]octane ring and legs of the cap as well as pyrrolic and phenylic protons of the tetraphenylporphyrin moiety confirm that the bridge of the bicyclo[2.2.2]octane keystone points upward and away from the porphyrin ring. As such 2-H will be close to 1′-H and 6″-H to 3′-H (Figure 2). This is consistent with the low chemical shift of the 2-H and with the relatively big difference in the chemical shifts of the 4′a-H and 4′b-H protons caused by the deshielding and shielding effect of the porphyrin ring, respectively.

Assuming that proton–proton interactions can be described by the same correlation time, the ROESY peaks can be related to the sixth power of the distance between protons involved in interactions[20] (Experimental Section, eq 3). Average distances were calculated for 12 interactions taking the separation of 1-H and 7-H of the bicyclo[2.2.2]octane ring to be that (2.402 Å) obtained by energy minimization of **VIAH$_2$**.[21] An angle of ~15° between the four phenyl rings and the porphyrin plane (assuming both the *meso* carbons are part of this plane) is required by the 2.45-Å distance between the 3″-H of the phenyl rings and β-pyrrolic hydrogens. The orientation of the 4′-H and 3′-H is defined by the distance of 2.50 Å between 3′-H and 6″-H. The constrains between 2-H and 1′a-H, 1′b-H and between 2′a-H, 2′b-H and 1′a-H, 1′b-H define the geometry of the legs. The distances between protons from ROESY are shown in Table III.

Distance Geometry (DGEOM) Calculations. An initial structure of **VIAH$_2$** was constructed with the computer program QUANTA and energy minimized in CHARM$_m$ (Polygen Corp.[21]). The coordinates of this minimized structure of **VIAH$_2$** were entered

---

(20) Kessler, H.; Bats, J. W.; Griesinger, C.; Koll, S.; Will, M.; Wagner, K. *J. Am. Chem. Soc.* **1988**, *110*, 1033.

(21) Quanta, Version 3.2.3; CHARMm, version 21.3; Polygen Corp., Waltham, MA, 1991. See: Brooks, B. R.; Bruccoleri, R. E.; Olafson, B. D.; States, D. J.; Swaminathan, S.; Karplus, M. *J. Comput. Chem.* **1983**, *4*, 187.

Table III. Experimental and Calculated Distances for **VIAH$_2$** (Å)

H–H	exp^a	calculation^b leg A	leg B	leg C	leg D	ϵ,^{c} %
3″–β (or β′)	2.447	2.971	2.913	3.375	*2.598*^{d}	6
4″–5″	2.610	2.484	2.486	2.483	*2.482*	−5
6″–3′	2.497	3.025	4.093	3.201	*2.517*	0.8
1′a–3′a	2.040	*2.292*	2.977	2.561	2.324	12
2′a–1′a	2.723	2.768	3.057	*2.603*	2.748	−4
2′b–1′a	2.732	3.007	*2.590*	3.055	3.044	−5
1–9b	2.569	2.411	2.314	2.405	*2.285*	−11
7–9b	2.587	3.058	*2.456*	2.997	2.640	−5
7–9a	2.621	3.456	2.750	*2.434*	2.633	−7
2–1	2.410	2.504	2.554	*2.500*	2.578	4
1–7	2.402^e	*2.351*	2.510	2.369	2.499	−2
2–1′a	2.356	3.699	*2.462*	3.658	3.549	4
2–1′b	2.483	2.311	3.771	*2.178*	3.986	−12
1–1′a	2.585	5.222	*2.597*	5.078	3.672	0.5

^{a} From ROESY data (25 °C, $CDCl_3$). ^{b} From the most stable conformer, see text. ^{c} $\epsilon = (d_C - d_R)/d_R$ where d_C is the shortest calculated distance and d_R is the ROESY distance. ^{d} The shortest calculated distance (d_C) is given in italics. ^{e} Distance from energy minimization and as a standard.

into the DGEOM program[22] along with the 12 distance constraints derived from the ROESY data (Table III). The upper bond distances were set 10–15% higher than the NMR distances allowing such that the lower bond distances equal the van der Waals distance separations. We did not include β (or β′)-H and 3″-H distance constraints because β (or β′)-H are not well enough resolved to assign accurately the NOE buildup to one of them. Because of the ruffling of the porphyrin ring due to the four *meso*-phenyl substituents,[23] the β-H and β′-H are not equivalent. Even though the resonances of these two kinds of protons can be resolved in the 1D spectrum, they appear in the ROESY 2D spectrum as overlapping cross-peaks. We also omitted the constraints between H-4″ and H-5″ because of uncertainty in the quantitation of the ROESY data.

One-hundred conformers of **VIAH$_2$**, which fit the ROESY constraints, were generated by use of the DGEOM program. By use of the DGEOM subprogram COMPARE there was generated a symmetric 100 × 100 matrix of least-squares rotation/translation fit root mean square (RMS) errors. The RMS matrix was subjected to a cluster analysis[24] which allowed the choice of grouping of the 100 conformers into thirteen conformational "families" using the statistical program Data Desk.[24] One representative conformer was chosen from each "family" and energy minimized (Table IV). The spread in energy content for the 13 minimized conformers is about 10 kcal/mol. The most stable conformer with $E = -20.12$ kcal/mol was mapped and the core size was determined within van der Waals distances.

It is found that the total energy of the minimized conformers is contributed to primarily by electrostatic and van der Waals terms (Table IV). The degree of ruffling of the porphyrin ring can be defined by the use of two dihedral angles.[23] In this study we have defined α as the dihedral angle between the plane of opposite pyrrole rings ($C_{\alpha i}C_{\alpha' i}$–$C_{\alpha j}C_{\alpha' j}$) and β as the angle between the porphyrin plane and the pyrrole planes. The total energy is associated with the nonplanarity of the porphyrin ring (Table IV), and we found that there is some correlation between the total energy and the tilting (β) and the twisting (α) of the pyrrole ring which act in opposite directions. An illustration of arbitrary linear plots of energy vs α and β is not shown.

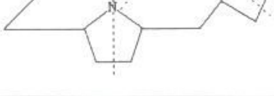

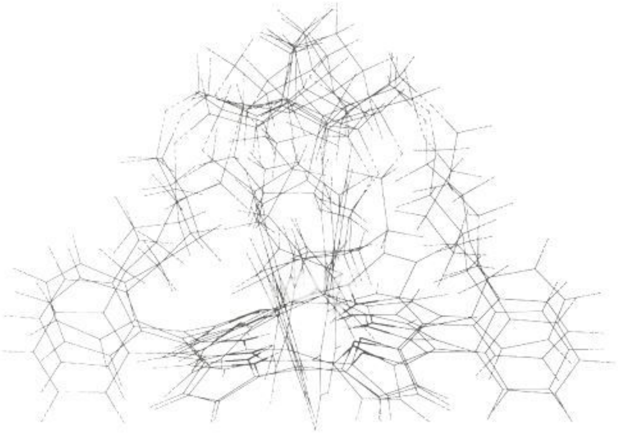

Figure 3. Overlapping of four representative conformations of the 13 chosen DGEOM minimized structures of **VIAH$_2$** (#74 (the most stable one), $E = -20.12$ kcal/mol; #59, $E = -16.20$ kcal/mol; #38, $E = -13.36$ kcal/mol, and #18, $E = -10.33$ kcal/mol) as a comparison of the nonplanarity of the porphyrin ring.

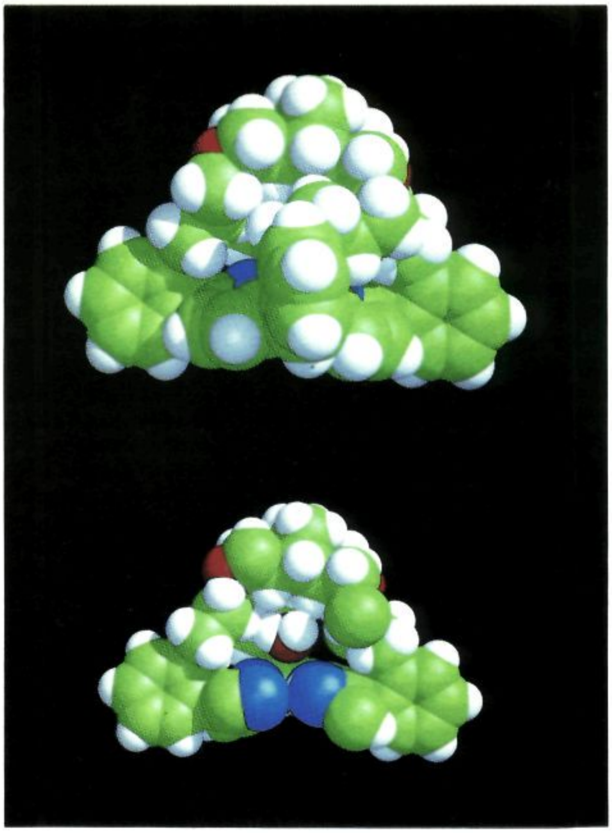

Figure 4. Top: A CPK presentation of the ROESY–DGEOM 3-dimensional structure of the most stable conformer of **VIAH$_2$** (conformer #74) in $CDCl_3$ at 25 °C. To the computer-generated structure of **VIAH$_2$** (QUANTA[21] see Experimental Section) there were added 42 ROESY distance constraints. One-hundred structures complying with these constraints were created by Distance Geometry.[22] Of the 100 DGEOM structures, 13 representatives were chosen by use of the statistical program Data Desk[24] and minimized in CHARMm.[21] The energetically most stable conformation is shown. Inspection of the structure shows that the bicyclo[2.2.2]octane "keystone" approaches the porphyrin by a twisting motion such that the four legs attaching the "keystone" to the porphyrin have a spiral shape. Bottom: A *yOz* cross section of the CPK ROESY–DGEOM 3-dimensional structure of the most stable conformer of **VIAH$_2$**. An H_2O molecule has been fitted into the cavity created by the capping structure in order to assist in visualization of the size of the cavity.

---

(22) Blaney, J. M.; Crippen, G. M.; Dearing, A.; Dixon, J. S. Du Pont de Nemours & Co., 1990.

(23) Shelnut, J. A.; Medforth, C. J.; Berber, M. D.; Barkigia, K. M.; Smith, K. M. *J. Am. Chem. Soc.* **1991**, *113*, 4077.

(24) Data Desk, Version 3.0: Odesta Corp., Northbrook, IL, 1989.

Table IV. Minimized Energies and Degree of Ruffling in the Representative Conformers Generated by DGEOM

compd	energy^a								
no.	total	dihedr angle	electrostatic	VDW	bond	impr tortion	angle	α^b	β^b
18	-10.33	28.61	-85.65	12.58	8.10	0.78	25.26	5.58	31.98
24	-12.45	28.55	-92.91	16.14	8.51	0.93	26.32	3.78	18.87
35	-13.40	26.97	-93.15	18.10	8.51	1.08	25.10	8.59	20.45
38	-13.36	29.40	-90.53	11.31	8.24	0.86	27.35	0.61	27.56
52	-12.79	31.27	-87.87	9.93	8.17	0.33	25.37	7.80	31.50
55	-12.42	28.76	-90.38	15.09	8.14	0.64	25.33	0.52	16.54
58	-10.81	33.89	-87.89	7.20	8.15	0.86	27.00	5.82	32.48
59	-16.20	30.47	-92.43	9.01	8.51	0.69	27.56	11.04	26.97
60	-9.64	31.61	-88.44	11.52	8.11	0.82	26.75	1.02	33.19
74	-20.12	29.70	-91.77	6.88	8.17	0.28	26.62	13.54	15.64
84	-11.41	30.18	-89.93	15.14	8.16	0.30	24.75	6.58	29.21
88	-15.23	28.09	-91.95	14.46	8.22	0.19	25.77	1.83	25.93
91	-10.47	27.99	-89.10	16.61	8.18	0.32	25.53	8.94	31.10

^{a}In kcal/mol. ^{b}As mean value, in deg.

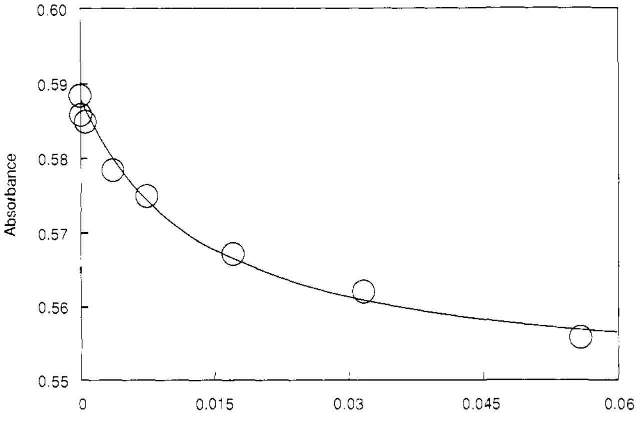

Figure 5. The change in absorbance at 508 nm which accompanies the titration of $[(\mathrm{IVA})\mathrm{Fe^{III}}]^+(\mathrm{SbF_6})^-$ (1.00×10^{-4}) by *N*-methylimidazole (toluene solvent at 25 °C). The points are experimental and the line is generated from eq 2 with the use of $K = 71\ \mathrm{M^{-1}}$.

The refined distance values for the most stable minimized DGEOM conformer are consistent with the NMR data (Table III). The differences between the calculated H-H distances for legs A and D come from the substituent-induced nonplanarity of the porphyrin ring which modifies the relative position of the adjacent phenyl rings (see central phenyl rings in Figure 3) and consequently those of the legs' segments. The shortest H-H distance has the major contribution to the ROESY peaks buildup because the signal decreases with the sixth power of the H-H distance (eq 3, see Experimental Section). Therefore, the calculated deviation (ϵ of Table III) is within 12%.

The three-dimensional structure (Figure 4) of **VIAH$_2$** determined by these techniques shows a spiral shape of the cap and a ruffled structure of the porphyrin ring. These features allow the exposure of a minimum of surface of the molecule to the $\mathrm{CDCl_3}$ solution.

The Cavity Size for VIAH$_2$. The eventual use of the capped porphyrin structure **VIAH$_2$** will be as a portion of a synthetic device when it ligates a metal cation. The core size of **VIAH$_2$** will determine what solvent or anions can fit under the cap. A water molecule may be used to visually appreciate the volume of the cavity. Examination of conformers shows that the size of the cavity of the conformers increases with an increase in total energy. However, only one water molecule can be fit into the cavities from the most stable conformer (Figure 5) to the less stable conformers.

Synthesis and Characterization of Ferric Capped Porphyrins. Reaction of **VIAH$_2$** with anhydrous ferrous chloride in dry chlorobenzene under reflux for 3 h (Ar atmosphere) provided the iron(III) ligated species **(VIA)Fe^{III}(Cl)** (**17**) in nearly quantitative yield.[25] Its visible absorption (375 nm) supports a porphyrinato iron(III) chloride structure. The molecular weight by FABMS (1149) is in accord with the required empirical formula $\mathrm{C_{72}H_{74}ClFeN_4O_4}$. The ^{1}H NMR exhibits the existence of a highly down-shifted peak at δ 80.8 ppm characteristic of β-pyrrole protons of a porphyrin ring ligated to iron(III) in its high-spin state.[26] The antimony hexafluoride salt **(VIA)Fe^{III}(SbF$_6$)** (**18**) was prepared by adding silver hexafluoroantimonate to a solution of **(VIA)Fe^{III}(Cl)** in toluene under reflux.[27] On formation of **(VIA)Fe^{III}(SbF$_6$)**, the visible absorption of **(VIA)Fe^{III}(Cl)** at 375 nm disappears and the ^{1}H β-pyrrole resonances shift from δ 80.8 to 79.9 ppm. Therefore, iron(III) still remains in its high-spin state.

Five-Coordinate *N*-Methylimidazole Complex of [(VIA)Fe^{III}]$^+$. From the most stable conformer of **VIAH$_2$** it would appear that the capped side should be fully protected from the approach of any ligand larger than $\mathrm{H_2O}$. The protection of the porphyrin moiety by its cap has been investigated by observing the ligation of *N*-methylimidazole (MeIm) with $[(\mathrm{VIA})\mathrm{Fe^{III}}]^+(\mathrm{SbF_6})^-$ (eq 1) in dry toluene at 25 °C. The binding of nitrogen bases to iron(III) porphyrins is quite favorable such that studies of the reaction of imidazole with most ferric porphyrins have involved observations made on bis-imidazole complexes.[28] Equilibrium constants for mono-imidazole ligation of an iron(III) porphyrin has only recently been reported.[28e] The formation of $[(\mathrm{VIA})\mathrm{Fe^{III}}(\mathrm{MeIm})]^+(\mathrm{SbF_6})^-$ was monitored by the visible spectral changes as an increasing amount of MeIm was added to a solution of **18**. A clear isosbestic point was observed near 524.5 nm and therefore there were only two species, free iron(III) porphyrin and mono-ligation complex, in the solution even when a large excess of MeIm was used. A plot of A_{508} vs [MeIm] is shown in Figure 5. The points of Figure 5 are experimental and the line connecting the points was determined by nonlinear least-squares iterative fitting using eq 2 where A_0 is the absorbance of the porphyrin solution in the absence of MeIm and A_∞ the absorbance of the solution when the iron(III) porphyrin is saturated with ligand. A value of 71 M^{-1} was determined for the equilibrium constant of eq 2. The small value of K is in accord with previous approximations of imidazole mono-ligation of simple tetraphenylporphyrin derivatives in organic solvents.[28]

$$[(\mathrm{VIA})\mathrm{Fe^{III}}]^+(\mathrm{SbF_6})^- + \mathrm{MeIm} \overset{K}{\rightleftharpoons} [(\mathrm{VIA})\mathrm{Fe^{III}}(\mathrm{MeIm})]^+(\mathrm{SbF_6})^- \tag{1}$$

$$A_{508} = \frac{A_0 + A_\infty K[\mathrm{MeIm}]}{1 + K[\mathrm{MeIm}]} \tag{2}$$

Conclusion

The goal of the present study has been to develop the capacity to synthesize tetraphenylporphyrins whose structures satisfy certain

---

[25] Landergen, M.; Baltzer, L. *Inorg. Chem.* **1990**, *29*, 556-557.

[26] (a) La Mar, G. N. *J. Am. Chem. Soc.* **1972**, *94*, 8606-8607. (b) Behere, D. V.; Birdy, R.; Mitra, S. *Inorg. Chem.* **1982**, *21*, 386-390.

[27] (a) Quinn, R.; Nappa, M.; Valentine, J. S. *J. Am. Chem. Soc.* **1982**, *104*, 2588-2595. (b) Reed, C. A.; Mashiko, T.; Bentley, S. P.; Kastner, M. E.; Scheidt, W. R.; Spertalian, K.; Lang, G. *J. Am. Chem. Soc.* **1979**, *101*, 2948-2958.

criteria that would allow their employment as part of certain redox devices. (i) The attachment of the cap to the tetraphenylporphyrin should not increase the susceptibility of the porphyrin moiety to oxidation, (ii) the most stable conformations should not allow approach of reagents to the capped face of the porphyrin, and (iii) the cavity formed between the cap and porphyrin plane should not exceed in volume that required for water or a small counterion. We have reached these goals in the synthesis of **VIAH$_2$** and the salts (**VIA**)Fe^{III}(X) {X = Cl$^-$ or SbF$_6^-$} which are attainable in reasonable percentage yields. ROESY experiments and Distance Geometry calculations have been used to identify the solution structures of the most stable conformations of **VIAH$_2$**. The cavity formed between the cap and porphyrin plane decreases with an increase in conformation stability due to a screwing down motion of the cap. With ordinary CPK models it can be shown that a forced extension of the cap to give the most unstable conformation allows accommodation of four H$_2$O molecules; however, the cavity of the four stable conformations (differing in stability by 10 kcal/mol) can accommodate only one H$_2$O molecule. Though ligation of two *N*-methylimidazoles (MeIm) to iron(III) tetraphenylporphyrins is thermodynamically favorable only one MeIm ligates with the iron(III) moiety of (**VIA**)**Fe^{III}**(**SbF$_6$**). Examination of **VIAH$_2$** with ordinary CPK models forcibly extended shows that it is impossible for ligation to occur on the capped side of the porphyrin plane with bases such as MeIm.

Experimental Section

Melting points were obtained on a Laboratory Devices Mel-Temp apparatus and are uncorrected. R_f values were obtained on E. M. Sciences 0.25 mm thick precoated glass-backed silica gel 60 F-254 plates. IR spectra were recorded on a Perkin-Elmer 1330 spectrophotometer. Mass spectra were obtained using electron impact (EI) and fast atom bombardment (FAB) mass spectroscopy with *m*-nitrobenzyl alcohol as the matrix and a parallel run of cesium rubidium iodide for the reference. Exact mass spectra was obtained using PFK as a reference compound. High-resolution fast atom bombardment mass spectroscopy (HRFABMS) was performed by the Midwest Center for Mass Spectrometry at the University of Nebraska-Lincoln. Elemental analyses were performed by Galbraith Laboratories, Knoxville, Tennessee. UV/Vis spectra were obtained on an OLIS Cary-14 Spectrophotometer at 25 °C in chloroform, unless otherwise specified. All reactions were carried out with purified reagents in dry, purified solvents[29] under an atmosphere of argon unless noted otherwise. Column chromatography was performed with Fischer type 60A (200–425 mesh) silica gel. HPLC analysis was carried out using an Alltech RSTI CN 5 mm column, a Perkin-Elmer Series 10 pump, a Hewlett-Packard variable wavelength detector (Model HP 1050), a Hewlett-Packard integrator (Model 3392A), and a Rheodyne injector (Model 7125).

NMR experiments were recorded at 500 MHz on a General Electric GN-500 spectrometer at 25 °C in CDCl$_3$. Chemical shifts were reported relative to the signal of CHCl$_3$ (^{1}H, 7.240 ppm, ^{13}C, 77.000 ppm). Deuterium exchange experiments were run in CDCl$_3$ with addition of 1% D$_2$O. Phase-sensitive double-quantum filtered COSY spectra were recorded using the pulse sequence[30a] $90°–t_1–90°_{\Phi1}–\Delta–90°_{\Phi2}$–aquisition$_{\Phi R}$ with 90° pulse of 12.2 μs calibrated before experiment, and Δ = 8 μs and an eight-step phase cycling has been applied.[31] Spectra were collected into 4K data blocks for 256 t_1 increments with a relaxation delay of 1.5 s. The spectral width in both dimensions was 6172.83 Hz for **VIAH$_2$** and 6849 Hz for **VICH$_2$**. The data matrix was zero filled to 2K and apodized with an exponential function to give a line broadening of 1 Hz in both dimensions. 2D ^{13}C–^{1}H heteronuclear shift correlation data were recorded using the pulse sequences[30b] (^{1}H) $90°_{\Phi1}–t_1–\Delta_1–90°_{\Phi2}–t–\Delta2$–decouple (^{13}C) $t_{1/2}–180°_{\Phi1}–t_{1/2}–\Delta1–t–90°_{\Phi3}–\Delta2$–aquisition$_{\Phi R}$ with a 90° (^{13}C) pulse of 17.5 μs and 90° (^{1}H) pulse of 32 μs calibrated before the experiment and with an eight-step phase cycling[30c] to afford qadrature detection in both frequency domains. Spectra were collected into 4K data blocks for 256 t_1 increments with a relaxation delay of 1.5 s, Δ1 = 3.2 ms, Δ2 = 2.1 ms, t = 10 μs. The spectral width in the first dimension was 4098.36 Hz and that in the second dimension was 18867.92 Hz. The data matrix was zero filled to 1K and apodized with a double exponential function to give a line broadening of 3 Hz in both dimensions. ROESY spectra were collected using the Kessler pulse sequence[32] $90°_x–t_1–(\beta_y–\tau)_n$–aquisition. The sample was degassed with argon and sealed. Spectra were collected into 4K data blocks for 512 t_1 increments with a relaxation delay of 3 s, β = 30°, τ = 3 ms, n = 7491, 5618, 1873 to give a mixing time of 200, 150, and 50 μs with a locking field of 4.6 kHz and spectral width in both dimensions of 6711.70 Hz. The data matrix was zero filled to 2 K and apodized with a Gaussian function to give a line broadening in both dimensions of 4 Hz. The 2D spectrum was reversed to transform the negative ROESY peaks into positive ones and the volume integrals of the peaks were measured. Quantitative data were obtained using eq 3, which includes also the offset correction

$$r^6_{\mathrm{ab}} = K \sin^2 (\beta_{\mathrm{a}}) \sin^2 (\beta_{\mathrm{b}})/I_{\mathrm{ab}}$$

$$\beta_{\mathrm{i}} = \mathrm{arctg}\,(\gamma B_1/\omega_{\mathrm{i}}) \qquad (3)$$

where r_{ab} is the distance between protons a and b, B_1 is the field strength of the locking field, γ is the magnetogyric ratio, ω_{i} is the resonance offset of nucleus i, and K is a constant evaluated from the cross-peak volume integral I_{ij} of protons i and j with known separation.

Distance Geometry. The porphyrin structures were built and minimized on a Silicon Graphics IRIS 4D/220 GTX workstation using the programs Quanta, Version 3.2.3, and CHARMm, Version 21.3 (Polygen Corp.).[20] The topology file PORPHYRIN.RTF was supplied by Polygen and the linkers were constructed in ChemNote, the 2D modeling facility in Quanta. Minimizations were performed in CHARMm until the energy change tolerance was less than 10^{-9} kcal/mol. The Distance Geometry (DGEOM) program was supplied by Du Pont de Nemours and uses an algorithm already reported.[33] The ROESY distance constraints were input using a constraints file and the RMSFIT.MATRIX was cluster analyzed using a program Data Desk[24] (Odesta Corp.).

Tetraethyl Bicyclo[2.2.2]octane-2-*syn*,3-*syn*,5-*syn*,6-*syn*-tetracarboxylate (2). A mixture of tetraethyl bicyclo[2.2.2]oct-7-ene-2-*syn*,3-*syn*,5-*syn*,6-*syn*-tetracarboxylate[15] (10.0 g) and 5% Pd/C (1.0 g) in ethyl acetate (400 mL) was degassed in vacuum and then hydrogen was introduced. The reaction was stirred at room temperature under 1 atm of hydrogen for 48 h. The catalyst was removed by passing through a silica gel column (20 g) and eluted with an additional 400 mL of ethyl acetate. Evaporation of solvent gave a solid product (10.0 g, quantitatively) which recrystallized from ethanol (50 mL) to yield 8 g of **2** as white needles. Mp 126–128 °C. R_f = 0.37 (25% ethyl acetate/hexanes). IR: 2940, 1715, 1360, 1270, 1175 cm^{-1}. ^{1}H NMR: δ 1.210 (t, 12 H, J = 7.5 Hz, CH$_3$ in ethyl esters), 1.668 (s, 4 H, 7,8-H), 2.529 (s, 2 H, 1,4-H), 2.855 (s, 4 H, 2,3,5,6-H), 4.0–4.15 (m, 8 H, CH$_2$ in ethyl esters) ppm. ^{13}C NMR: δ 14.0 (methyl in ethyl esters), 16.9 (7,8-C), 29.4 (1,4-C), 43.8 (2,3,5,6-C), 60.4 (methylene in ethyl esters), 172.3 (carbonyl) ppm. MS: m/z (relative intensity) 398 (M$^+$, 1.4), 353 [(M – OEt)$^+$, 100], 306 (50), 278 (19), 251 (26), 232 (16). Anal. Calcd for C$_{20}$H$_{30}$O$_8$: C, 60.29; H, 7.59. Found: C, 60.21; H, 7.86.

2-*syn*,3-*syn*,5-*syn*,6-*syn*-Tetrakis(hydroxymethyl)bicyclo[2.2.2]octane (3).[14] A solution of **2** (20.0 g, 50.2 mmol) in anhydrous THF (180 mL) was added dropwise to a vigorously stirred suspension of lithium aluminum hydride (5.6 g, 150 mmol, Aldrich) in dry THF (180 mL) during 1 h. After the addition, the mixture was stirred and heated under reflux for 16 h. After cooling, a mixture of water (10 mL) and THF (50 mL) was added dropwise and the reaction mixture was refluxed for 1 h. The mixture was filtered through silica gel (20 g), and the precipitate formed was stirred with the silica gel in boiling ethanol (500 mL) for 12 h and then filtered through another portion of silica gel (20 g). The combined organic layer was concentrated in vacuum to give a solid product which recrystallized from ethanol (75 mL) to afford **3** as white crystals (8.6 g, 75%). Mp 165–167 °C (lit. mp[14] 158–160 °C). ^{1}H NMR (DMSO-d_6):

---

(28) (a) Balke, A. D.; Walker, F. A.; West, J. T. *J. Am. Chem. Soc.* **1985**, *107*, 1226. (b) Walker, G. A.; Lo, M.-W.; Ree, M. T. *J. Am. Chem. Soc.* **1976**, *98*, 5552. (c) Satterlee, J. D.; La Mar, G. N.; Frye, J. S. *J. Am. Chem. Soc.* **1976**, *98*, 7275. (d) Byers, W.; Cossham, J. A.; Edwards, J. O.; Gorden, A. T.; Jones, J. G.; Kenny, E. T. P.; Mahmood, A.; McKnight, J.; Sweigart, D. A.; Tondreau, G. A.; Wright, T. *Inorg. Chem.* **1986**, *25*, 4767. (e) Beck, M. J.; Gopinath, E.; Bruice, T. C. Manuscript in preparation.

(29) Perrin, D. D.; Perrin, D. R.; Armarego, W. L. F. *Purification of Laboratory Chemicals*; Pergamon Press: Oxford, 1980.

(30) Martin, G. E.; Zekter, A. S. *Two Dimensional NMR Methods for Establishing Molecular Connectivity*; VCH Publishers: New York, 1988; (a) p 199, (b) p 178, (c) p 180.

(31) (a) Wokaun, A.; Ernst, R. R. *Chem. Phys. Lett.* **1977**, *52*, 487. (b) Morris, A. *Magn. Reson. Chem.* **1986**, *24*, 371.

(32) Kessler, H.; Griesinger, C.; Kerssebaum, R.; Wagner, E.; Ernst, R. *J. Am. Chem. Soc.* **1987**, *109*, 607.

(33) (a) Crippen, G. M. *Distance Geometry and Conformational Calculations*; Bawden, D., Ed.; Research Studies Press, John Wiley: New York, 1981. (b) Havel, T. F.; Kunoto, I. D.; Crippen, G. M. *Bull. Math. Biol.* **1983**, *45*, 665.

δ 1.281 (s, 4 H, 7,8-H), 1.627 (s, 2 H, 1,4-H), 1.827 (s, 4 H, 2,3,5,6-H), 3.30–3.34 (m, 4 H, 9,11-H), 3.66–3.69 (m, 4 H, 10,12-H), 4.45–4.48 (m, 4 H, 4 × OH) ppm. Anal. Calcd for $C_{12}H_{22}O_4$: C, 62.58; H, 9.63. Found: C, 62.57; H, 9.86.

2-[2′-(4″-Bromobutyl)]phenyl-1,3-dioxolane (5). Magnesium turnings (Aldrich, 3.1 g, 128 mmol) were placed in a 250-mL three-necked flask and flame dried under vacuum. Argon was introduced and 3 pieces of crystals of iodine were added. Dry THF (150 mL) was added, the flask was warmed to 70–80 °C, and then **4** (3.0 mL) was added in one portion for initiating the reaction. The other portion of **4** (10.0 mL, totally 13.0 mL, 20.0 g, 87.3 mmol) was added at such a rate that the reaction proceeds smoothly (over a period of 40 min). After addition, the mixture was refluxed for an additional 1 h. The solution was titrated with *o*-phenanthroline/2-butanol and found to be 0.57 M in Grignard reagent.

To a solution of cuprous bromide (800 mg, 5.6 mmol), dry hexamethylphosphoramide (HMPA 10 mL), THF (25 mL), and 1,4-dibromobutane (10.0 mL, 18.1 g, 83.7 mmol) was added quickly a solution of Grignard reagent prepared as above (80 mL, 45.6 mmol) under argon with reflux and then the reaction mixture was kept under reflux for 3 h. The reaction mixture was cooled down to room temperature and water (30 mL) and aqueous saturated ammonium chloride solution (20 mL) were added. After workup with standard procedure[34] (2 × 300 mL of 50% ether/hexanes), vacuum distillation of the crude product gave **5** as a pale yellow liquid (10.9 g, 83%). Bp 129–131 °C (0.04 mmHg). R_f = 0.37 (10% ethyl acetate/hexanes). ^{1}H NMR: δ 1.74–1.80 (m, 2 H, 2″-H), 1.90–1.96 (m, 2 H, 3″-H), 2.750 (t, 2 H, *J* = 8.0 Hz, 1″-H), 3.323 (t, 2 H, *J* = 7.0 Hz, 4″-H), 4.00–4.15 (m, 4 H, 4-H and 5-H), 5.975 (s, 1 H, 2-H), 7.170 (d, 1 H, *J* = 7.5 Hz, 3′-H), 7.214 (t, 1 H, *J* = 7.5 Hz, 5′-H), 7.278 (dt, 1 H, *J* = 7.5 and 1.0 Hz, 4′-H), 7.524 (d, 1 H, *J* = 7.5 Hz, 6′-H) ppm. ^{13}C NMR: δ 29.6, 30.9, 32.2, 33.4, 64.9 (4-C and 5-C), 101.2 (2-C), 125.7 (4′-C), 126.0 (3′-C), 128.7 (5′-C), 129.2 (6′-C), 134.7 (1′-C), 140.2 (2′-C) ppm. IR: 2910, 2850, 1590, 1560, 1440, 1380, 1090, 1060, 930, 740 cm^{-1}. MS: *m/z* 286 [(M + 2)$^+$, 24%], 285 [(M + 1)$^+$, 35], 284 [(M)$^+$, 25], 283 [(M − 1)$^+$, 33], 241 [(M − $C_2H_4O_2$ + 2)$^+$, 8], 239 [(M − $C_2H_4O_2$)$^+$, 8], 149 [(M − C_4H_8Br)$^+$, 92], 73 (dioxolanyl, 100). Exact mass: 286.0365 (calcd for $C_{13}H_{17}{}^{81}BrO_2$: 286.0391).

***2-syn,3-syn,5-syn,6-syn*-Tetrakis{4′-[2″-(1‴,3‴-dioxolan-2‴-yl)-phenyl]butoxymethyl}bicyclo[2.2.2]octane (6).** Potassium hydride (1.74 g of 50 wt %,[35] 21.7 mmol) and **3** (598 mg, 2.60 mmol) were weighed into a predried 25-mL flask. Anhydrous HMPA (10 mL) was added under argon and the mixture was stirred for 10 min. The bromide **5** (3.0 mL, 4.0 g, 14 mmol) was added dropwise during 30 min with vigorous stirring and at a temperature between 40 and 50 °C. After addition, the mixture was stirred for 1 h. Ethanol (0.5 mL) was carefully added followed by addition of water (40 mL). The standard workup (2 × 200 mL of 25% dichloromethane/diethyl ether) procedure was used and then the solution was chromatographed on silica gel (20% diethyl ether/dichloromethane) to give 1.83 g of oily product **6** (67% of yield). R_f = 0.44 (20% diethyl ether/dichloromethane). ^{1}H NMR:[36a] δ 1.400 (s, 4 H, 7,8-H), 1.55–1.68 (m, 16 H, 2′-H and 3′-H), 1.699 (s, 2 H, 1,4-H), 2.098 (s, 4 H, 2,3,5,6-H), 2.717 (t, 8 H, *J* = 7.5 Hz, 4′-H), 3.32–3.44 (m, 12 H, 9,11-H and 1′-H), 3.55–3.62 (m, 4 H, 10,12-H), 3.95–4.12 (m, 16 H, 4‴-H and 5‴-H), 5.964 (s, 4 H, 2‴-H), 7.152 (d, 4 H, *J* = 7.5 Hz, 6″-H), 7.177 (t, 4 H, *J* = 7.5 Hz, 4″-H), 7.241 (dt, 4 H, *J* = 7.5 and 1.0 Hz, 5″-H), 7.524 (d, 4 H, *J* = 7.5 Hz, 3″-H) ppm. ^{13}C NMR:[36a] δ 16.1 (7,8-C), 28.1 and 29.6 (2′-C and 3′-C), 29.1 (1,4-C), 31.9 (4′-C), 38.5 (2,3,5,6-C), 65.2 (4‴-C and 5‴-C), 70.2 (9,10,11,12-C), 70.6 (1′-C), 101.4 (2‴-C), 125.8 (4″-C), 126.0 (3″-C), 128.9 (5″-C), 129.5 (6″-C), 134.9 (1″-C), 141.1 (2″-C) ppm. IR: 2930, 2850, 1600, 1580, 1450, 1390, 1215, 1100, 940, 750 cm^{-1}. FABMS: *m/z* 1047 (M + 1)$^+$, 1046 (M)$^+$.

***2-syn,3-syn,5-syn,6-syn*-Tetrakis{4′-[2″-formylphenyl]butoxymethyl}bicyclo[2.2.2]octane (7).** A mixture of **6** (1.70 g, 1.62 mmol) and pyridinium *p*-tosylate (500 mg) in 5% water/acetone (160 mL) was refluxed for 16 h under argon. The solvent was evaporated and the residue was followed by the standard workup procedure (100 mL of 25% dichloromethane/diethyl ether). Chromatography on silica gel (14% diethyl ether/dichloromethane) gave an oily product **7** (1.20 g, 85%). R_f = 0.30 (14% diethyl ether/dichloromethane). ^{1}H NMR:[36b] δ 1.376 (s, 4 H, 7,8-H), 1.55–1.65 (m, 16 H, 2′-H and 3′-H), 1.669 (s, 2 H, 1,4-H), 2.069 (s, 4 H, 2,3,5,6-H), 2.986 (t, 8 H, *J* = 7.0 Hz, 4′-H), 3.30–3.40 (m, 12 H, 1′-H and 9,11-H), 3.52–3.57 (m, 4 H, 10,12-H), 7.217 (d, 4 H, *J* = 7.5 Hz, 6″-H), 7.299 (t, 4 H, *J* = 7.0 Hz, 4″-H), 7.438 (dt, 4 H, *J* = 7.0, 1.0 Hz, 5″-H), 7.769 (dd, 4 H, *J* = 7.5, 1.0 Hz, 3″-H), 10.219 (s, 4 H, aldehyde) ppm. ^{13}C NMR:[36b] δ 16.0 (7,8-C), 28.9 (3′-C), 29.1 (1,4-C), 29.5 (2′-C), 32.2 (4′-C), 38.5 (2,3,5,6-C), 70.2 (9,10,11,12-C), 70.6 (1′-C), 126.4, 131.0, 131.6, 133.65, 133.70, 145.3 (benzene rings), 192.2 (aldehyde) ppm. IR: 2920, 2850, 2730, 1686, 1595, 1570, 1480, 1445, 1205, 1185, 1105, 775 cm^{-1}. FABMS: *m/z* 871 (M + 1)$^+$, 870 (M)$^+$.

C4 Capped Porphyrin VIAH$_2$. To a solution of **6** (633 mg, 0.604 mmol) in chloroform (commercial, 1350 mL) were added pyrrole (0.168 mL, 2.40 mmol) and boron trifluoride etherate (0.446 mL, 3.62 mmol) under argon. The reaction was stirred for 20 h at room temperature in the dark. DDQ (600 mg) was added and the solution was refluxed for 1 h when another portion of DDQ (600 mg) was added. The solution was refluxed for an additional 2 h. The appearance of porphyrin was monitored by UV/vis at 420 nm. The solvent was removed by rotary evaporator, and the residue was dissolved in dichloromethane (10 mL) and then silica gel (5 g) was added. After drying, the silica gel was placed on the top of a silica gel column and chromatographed by eluting with 25% ethyl acetate/hexanes. The porphyrin portions were collected and once again chromatographed over a silica gel column (eluted with 14% diethyl ether/dichloromethane). Removal of the solvent gave pure VIAH$_2$ as purple plates (70 mg, 11%). Mp >300 °C. R_f = 0.36 (25% ethyl acetate/hexanes), 0.33 (14% diethyl ether/dichloromethane). ^{1}H NMR: see Table II. ^{13}C NMR:[37] δ 13.4 (7,8-C), 26.0 (2′-C), 26.4 (1,4-C), 26.5 (3′-C), 30.8 (4′-C), 33.7 (2,3,5,6-C), 66.5 (9,10,11,12-C), 68.6 (1′-C), 119.1 (*meso*), 123.7 (5″-C), 127.5 (3″-C), 128.5 (4″-C), 130.9 (br, β), 134.6 (6″-C), 141.7 (1″-C), 143.1 (2″-C) ppm. IR: 3270 (N–H), 2880, 2810, 1450, 1330, 1100, 950, 785, 735 cm^{-1}. FABMS: *m/z* 1062 (M + 2)$^+$, 1061 (M + 1)$^+$. UV/vis (log ε): 368.5 (4.27), 420.0 (5.64), 481.5 (3.37), 515.5 (4.23), 549.0 (3.67), 592.5 (3.65), 646.5 (3.34) nm. HPLC: (a) one peak, R_t = 12.12 min (10% ethyl acetate-/hexanes, 1.0 mL/min, 420 nm); (b) one peak, R_t = 8.69 min (2% diethyl ether/dichloromethane, 1.5 mL/min, 420 nm). HRFABMS: *m/z* 1061.5946 [calcd for $C_{72}H_{77}N_4O_4$ (M + H)$^+$: 1061.5945].

2-[2′-(3″-Oxy-3″-methoxy)propyl]phenyl-1,3-dioxolane (9). Ozone was bubbled through a solution composed of **8**[18] (10.0 g, 62.4 mmol), pyridine (2 mL), and a catalytic amount of Sudan red 7B (2–3 mg as an indicator) in dichloromethane (100 mL) at −78 °C until the red color of the solution disappeared (about 1 h). Dimethyl sulfite (10 mL) was added at the same temperature and the solution was allowed to warm to room temperature. The reaction solution was stirred for 2 h and then washed with water (20 mL). After the standard workup (dichloromethane) procedure, a crude product of 2-(3′-oxy-3′-methoxypropyl)-benzaldehyde was afforded. ^{1}H NMR (CDCl$_3$, 300 MHz): δ 2.639 (t, 2 H, *J* = 7.8 Hz, CH_2COOR), 3.341 (t, 2 H, *J* = 7.8 Hz, benzylic), 3.640 (s, 3 H, CH_3O), 7.307 (d, 1 H, *J* = 7.2 Hz, 3′-H), 7.402 (t, 1 H, *J* = 7.2 Hz, 5′-H), 7.504 (t, 1 H, *J* = 7.8 Hz, 4′-H), 7.797 (d, 1 H, *J* = 7.8 Hz, 6′-H), 10.188 (s, 1 H, CHO) ppm. This crude product was dissolved in benzene (200 mL) and pyridinium *p*-tosylate (1 g) and ethylene glycol (10 mL) were added. The reaction solution was refluxed for 2 h followed by the standard workup (diethyl ether) procedure. Vacuum distillation of the crude product gave pure compound **9** as a colorless liquid (10.09 g, 68.4%): Bp 125–126 °C (0.08 mmHg). R_f = 0.31 (25% ethyl acetate/hexanes). ^{1}H NMR: δ 2.632 (t, 2 H, *J* = 8.0 Hz, 2″-H), 3.409 (t, 2 H, *J* = 8.0 Hz, 1″-H), 3.627 (s, 3 H, methoxy), 3.95–4.10 (m, 4 H, 4-H and 5-H), 5.939 (s, 1 H, 2-H), 7.168 (d, 1 H, *J* = 7.5 Hz, 3′-H), 7.200 (dt, 1 H, *J* = 7.5 and 1.5 Hz, 5′-H), 7.255 (dt, 1 H, *J* = 7.5 and 1.5 Hz, 4′-H), 7.524 (dd, 1 H, *J* = 7.5 and 1.5 Hz, 6′-H) ppm. ^{13}C NMR: δ 27.2 (2″-C), 35.5 (1″-C), 51.2 (CH_3O), 64.9 (4-C and 5-C), 101.6 (2-C), 126.1, 126.3, 129.0, 129.4, 134.9, 139.1 (benzene ring), 173.1 (3″-C) ppm. IR: 2940, 2875, 1724, 1596, 1575, 1430, 1200, 1160, 1070, 750 cm^{-1}. MS: *m/z* (relative intensity) 236 (M$^+$, 2), 235 [(M − H)$^+$, 7], 205 [(M − CH_3O)$^+$, 6], 162 [(M − H − CH_2COOMe)$^+$, 6], 149 [(M − CH_2CH_2COOMe)$^+$, 100], 133 (7), 132 (7), 131 (11), 117 (11), 105 (13), 73 (22). Exact mass: *m/z* 236.1042 (calcd for $C_{13}H_{16}O_4$: 236.1048).

2-[2′-(3″-Hydroxypropyl)]phenyl-1,3-dioxolane (10). To a solution of **9** (9.40 g, 39.8 mmol) in dry THF (100 mL) was added slowly a 1.0 M solution of lithium aluminum hydride in THF (26.0 mL, 26.0 mmol) under argon at 0 °C over 5 min. The mixture was stirred at 0 °C for 20 min. Methanol (2 mL) was added carefully at 0 °C and a saturated

---

(34) The standard workup procedure refers to extracting an aqueous solution with an adequate organic solvent, washing the extracts with water and brine, drying over anhydrous sodium sulfate, and evaporating the solvent by a rotary evaporator.

(35) 50 wt % of potassium hydride was made from 35 wt % of KH dispersion in mineral oil (Aldrich) by removal of some clear oil. The concentration of this remaining potassium hydride was determined by washing a given amount of mixture with dry hexanes three times under argon and weighing the pure potassium hydride.

(36) (a) Assignments are based on ^{13}C–^{1}H and ^{1}H–^{1}H 2D NMR. (b) Assignments are based on comparison with similar compounds.

(37) By comparison with the ^{13}C NMR spectrum of *meso*-tetra(*o*-tolyl)-porphyrin. See Abraham, R. J.; Hawkes, G. E.; Hudson, M. F.; Smith, K. M. *J. Chem. Soc. Perkin Trans. II* **1975**, 204–211.

solution of potassium sodium tartrate tetrahydrate (4 mL) was added. The mixture was stirred at room temperature for 1 h and then filtered through silica gel (10 g). The solid was washed with ethyl acetate four times (100 mL × 4) and the combined organic solvent was concentrated. Column chromatography on silica gel (150 g) gave an oily compound **10** (7.13 g, 86.1%). $R_f = 0.25$ (50% ethyl acetate/hexanes). ^{1}H NMR: δ 1.85–1.92 (m, 2 H, 2″-H), 2.382 (br, 1 H, OH), 2.818 (t, 2 H, *J* = 7.5 Hz, 1″-H), 3.552 (t, 2 H, *J* = 4.5 Hz, 3″-H), 3.95–4.15 (m, 4 H, 4-H and 5-H), 6.009 (s, 1 H, 2-H), 7.15–7.30 (m, 3 H, aromatic H), 7.541 (d, 1 H, *J* = 8.0 Hz, 6′-H) ppm. ^{13}C NMR δ 27.5 (2″-C), 34.1 (1″-C), 61.3 (3″-C), 65.2 (4-C and 5-C), 102.0 (2-C), 126.0, 126.2, 129.2, 129.6, 134.9, 140.4 (benzene ring) ppm. IR (NaCl plates): 3300–3400 (OH), 2950, 2850, 1600, 1550, 1390, 1210, 750 cm^{-1}. MS: *m/z* (relative intensity) 208 (M^+, 3.2), 207 [$(M - H)^+$, 13], 162 [$(M - C_2H_4OH)^+$, 6], 149 [$(M - C_3H_6OH)^+$, 100], 133 (11), 117 (40), 105 (20), 73 (52). Exact mass: *m/z* 207.1029 [calcd for $C_{12}H_{15}O_3$ $(M - H)^+$: 207.1021].

2-[2′-(3″-Bromopropyl)]phenyl-1,3-dioxolane (11). To a solution of **10** (1.84 g, 8.84 mmol) in dry pyridine (10 mL) was added dropwise mesyl chloride (1.03 mL, 13.2 mmol) at 0 °C under argon. The mixture was stirred at 0 °C for 1 h. Cold water (25 g) was added and the whole extract with ethyl acetate (100 mL). The organic layer was washed with saturated sodium bicarbonate (25 mL) and brine (25 mL) and dried over anhydrous sodium sulfate. After evaporating the solvent, the residue was treated with benzene three times for removing the residual pyridine. The crude mesylate was dissolved in dry acetone (30 mL) and a solution of tetra-*n*-butylammonium bromide (4.27 g, 13.3 mmol) in acetone (20 mL) was added under argon. The reaction mixture was refluxed for 90 min. After removal of most of the solvent, the residue was worked up with the standard procedure (200 mL of 10% ethyl acetate/hexanes). Column chromatography on silica gel (60 g, eluted with 10% ethyl acetate/hexanes) followed by distillation gave pure **11** as a colorless liquid (2.22 g, 93%). Bp 124–126 °C (0.05 mmHg). $R_f = 0.32$ (10% ethyl acetate/hexanes). ^{1}H NMR: δ 2.17–2.24 (m, 2 H, 2″-H), 2.922 (t, 2 H, *J* = 7.5 Hz, 1″-H), 3.450 (t, 2 H, *J* = 6.5 Hz, 3″-H), 3.97–4.16 (m, 4 H, 4-H and 5-H), 6.000 (s, 1 H, 2-H), 7.233 (dd, 1 H, *J* = 7.5 and 1.0 Hz, 3′-H), 7.272 (dt, 1 H, *J* = 7.5 and 1.0 Hz, 5′-H), 7.322 (dt, 1 H, *J* = 7.5 and 1.5 Hz, 4′-H), 7.615 (dd, 1 H, *J* = 7.5 and 1.5 Hz, 6′-H) ppm. ^{13}C NMR: δ 30.2 (2″-C), 33.4 (3″-C), 34.0 (1″-C), 64.9 (4-C and 5-C), 101.3 (2-C), 126.0, 126.3, 128.8, 129.5, 134.9, 139.1 (benzene ring) ppm. IR: 2940, 2870, 1600, 1575, 1390, 1215, 1100, 1065, 750 cm^{-1}. MS: *m/z* (relative intensity) 272 [$(M + 2)^+$, 20], 271 [$(M - H + 2)^+$, 35], 270 (M^+, 22), 269 [$(M - H)^+$, 33], 227 [$(M - OCH_2CH_2 + 2)^+$, 5], 225 [$(M - OCH_2CH_2)^+$, 6], 162 [$(M - H - CH_2CH_2Br)^+$, 4], 149 [$(M - C_3H_6Br)^+$, 87], 133 (6), 129 (33), 117 (28), 105 (18), 73 (dioxolanyl, 100). Anal. Calcd for $C_{12}H_{14}BrO_2$: C, 53.16; H, 5.58. Found: C, 53.06; H, 5.80.

2-*syn*,3-*syn*,5-*syn*,6-*syn*-Tetrakis{3′-[2″-(1‴,3‴-dioxolan-2‴-yl)phenyl]propoxymethyl}bicyclo[2.2.2]octane (12). Starting with **3** and **11**, an oily **12** was obtained in 77% yield by using the same procedure as in the preparation of **6**. $R_f = 0.41$ (20% diethyl ether/dichloromethane). ^{1}H NMR:[36a] δ 1.507 (s, 4 H, 7,8-H), 1.838 (s, 2 H, 1,4-H), 1.88–1.93 (m, 8 H, 2′-H), 2.191 (s, 4 H, 2,3,5,6-H), 2.811 (t, 8 H, *J* = 7.0 Hz, 3′-H), 3.40–3.50 (m, 12 H, 9,11-H and 1′-H), 3.65–3.68 (m, 4 H, 10,12-H), 3.96–4.12 (m, 16 H, 4‴-H and 5‴-H), 5.980 (s, 4 H, 2‴-H), 7.17–7.25 (m, 12 H, aromatic H), 7.550 (d, 4 H, *J* = 7.0 Hz, 3″-H) ppm. ^{13}C NMR:[36a] δ 16.1 (7,8-C), 28.7 (3′-C), 29.2 (1,4-C), 31.4 (2′-C), 38.7 (2,3,5,6-C), 65.1 (4‴-C and 5‴-C), 70.1 (9,10,11,12-C and 1′-C), 101.4 (2‴-C), 125.8 (4″-C), 126.1 (3″-C), 128.9 (5″-C), 129.6 (6″-C), 134.9 (1″-C), 140.6 (2″-C) ppm. IR: 2850, 1595, 1570, 1450, 1380, 1210, 1100, 1060, 750 cm^{-1}. FABMS: *m/z* 991 $(M + 1)^+$. Anal. Calcd for $C_{60}H_{78}O_{12}\cdot{}^1/_2CH_2Cl_2$: C, 70.29; H, 7.70. Found: C, 70.27; H, 7.46.

2-*syn*,3-*syn*,5-*syn*,6-*syn*-Tetrakis{3′-[2″-formylphenyl]propoxymethyl}bicyclo[2.2.2]octane (13). Deprotection of **12** gave an oily **13** in 87% yield by using the same procedure as in the preparation of **7**. $R_f = 0.56$ (20% diethyl ether/dichloromethane). ^{1}H NMR:[36b] δ 1.566 (s, 4 H, 7,8-H), 1.85–1.98 (m, 10 H, 1,4-H and 2′-H), 2.250 (s, 4 H, 2,3,5,6-H), 3.144 (t, 8 H, *J* = 7.5 Hz, 3′-H), 3.44–3.58 (m, 12 H, 1′-H and 9,11-H), 3.68–3.73 (m, 4 H, 10,12-H), 7.306 (d, 4 H, *J* = 7.5 Hz, 6″-H), 7.372 (t, 4 H, *J* = 7.0 Hz, 4″-H), 7.498 (t, 4 H, *J* = 7.5 Hz, 5″-H), 7.836 (d, 4 H, *J* = 7.0 Hz, 3″-H), 10.296 (s, 4 H, aldehyde) ppm. ^{13}C NMR:[36b] δ 16.0 (7,8-C), 28.8 (3′-C), 28.9 (1,4-C), 31.8 (2′-C), 38.5 (2,3,5,6-C), 69.6 and 69.9 (9,10,11,12-C and 1′-C), 126.3, 130.9, 131.4, 133.48, 133.53, 144.7 (benzene rings), 192.0 (aldehyde) ppm. IR: 2920, 2860, 2730, 1700, 1595, 1570, 1205, 1110, 750 cm^{-1}. FABMS: *m/z* 815 $(M + 1)^+$. Anal. Calcd for $C_{52}H_{62}O_8$: C, 76.62; H, 7.67. Found: C, 76.34; H, 7.65.

C3 Capped Porphyrin VIBH$_2$. VIBH$_2$ was prepared in 4% as purple plates from **12** by a procedure similar to that used in the preparation of **VIAH$_2$**. Mp >300 °C. $R_f = 0.36$ (25% ethyl acetate/hexanes), 0.33 (6.25% diethyl ether/dichloromethane). ^{1}H NMR: see Table II. ^{13}C NMR:[37] 13.4, 26.5, 29.7, 30.8, 65.3, 67.8, 119.0 (*meso*), 123.9 (5″-C), 128.3 (3″-C), 128.9 (4″-C), 130 (br, β-C), 136.7 (6″-C), 141.3 (1″-C), 143.7 (2″-C) ppm. IR: 3330 (N–H), 2940, 2870, 1820, 1735, 1605, 1560, 1475, 1358, 1120, 975, 810, 760, 740 cm^{-1}. FABMS: *m/z* 1006 $(M + 2)^+$, 1005 $(M + 1)^+$, 1004 $(M)^+$. UV/vis (log ε): 371.5 (4.16), 422.5 (5.44), 485.0 (3.25), 519.0 (4.06), 552.0 (3.56), 595.0 (3.48), 652.5 (3.32) nm. HRFABMS: *m/z* 1005.5319 [calcd for $C_{68}H_{69}N_4O_4$ $(M + H)^+$: 1005.5329].

2-*syn*,3-*syn*,5-*syn*,6-*syn*-Tetrakis{3′-[2″-(1‴,3‴-dioxolan-2‴-yl)phenyl]propoxymethyl}bicyclo[2.2.2]oct-7-ene (15). Starting with **14** and **11**, an oily **15** was obtained in 89% yield by using the same procedure as in the preparation of **6**. $R_f = 0.28$ (20% diethyl ether/dichloromethane). ^{1}H NMR:[36b] δ 1.85–1.95 (m, 8 H, 2′-H), 2.283 (s, 4 H, 2,3,5,6-H), 2.822 (dd, 8 H, *J* = 7.0 and 8.5 Hz, 3′-H), 2.906 (s, 2 H, 1,4-H), 3.175 (t, 4 H, *J* = 8.0 Hz, 10,12-H), 3.35–3.50 (m, 12 H, 9,11-H and 1′-H), 3.95–4.15 (m, 16 H, 4‴-H and 5‴-H), 5.997 (s, 4 H, 2‴-H), 6.233 (t, 4 H, *J* = 4.0 Hz, 7,8-H), 7.20–7.30 (m, 12 H, 4″-H, 5″-H, and 6″-H), 7.563 (d, 4 H, *J* = 7.0 Hz, 3″-H) ppm. ^{13}C NMR:[36b] δ 28.8 (3′-C), 31.5 (2′-C), 36.7 (1,4-C), 41.6 (2,3,5,6-C), 65.3 (4‴-C and 5‴-C), 70.1 (1′-C), 71.2 (9,10,11,12-C), 101.5 (2‴-C), 126.0 (4″-C), 126.2 (3″-C), 129.0 (5″-C), 129.7 (6″-C), 132.7 (7,8-C), 135.1 (1″-C), 140.7 (2″-C) ppm. IR: 2870, 1605, 1450, 1390, 1220, 1110, 1085, 945, 755 cm^{-1}. FABMS: *m/z* 989 $(M + 1)^+$.

2-*syn*,3-*syn*,5-*syn*,6-*syn*-Tetrakis{3′-[2″-formylphenyl]propoxymethyl}bicyclo[2.2.2]oct-7-ene (16). Deprotection of **15** gave an oily **16** in 88% yield by using the same procedure as in the preparation of **7**. $R_f = 0.46$ (20% diethyl ether/dichloromethane). ^{1}H NMR:[36b] δ 1.80–1.90 (m, 8 H, 2′-H), 2.235 (s, 4 H, 2,3,5,6-H), 2.861 (s, 2 H, 1,4-H), 3.061 (t, 8 H, *J* = 8.0 Hz, 3′-H), 3.114 (t, 4 H, *J* = 8.0 Hz, 10,12-H), 3.31–3.40 (m, 12 H, 9,11-H and 1′-H), 6.204 (t, 2 H, *J* = 4.0 Hz, 7,8-H), 7.232 (d, 4 H, *J* = 7.5 Hz, 6″-H), 7.303 (t, 4 H, *J* = 7.5 Hz, 4″-H), 7.426 (dt, 4 H, *J* = 7.5 and 1.0 Hz, 5″-H), 7.764 (d, 4 H, *J* = 8.0 Hz, 3″-H), 10.233 (s, 4 H, aldehyde) ppm. ^{13}C NMR:[36b] δ 28.9 (3′-C), 31.9 (2′-C), 36.4 (1,4-C), 41.4 (2,3,5,6-C), 69.6 (1′-C), 71.1 (9,10,11,12-C), 126.4, 131.0, 131.6, 133.6, 144.8 (benzene ring), 132.6 (7,8-C), 192.2 (aldehyde) ppm. IR: 2840, 1680, 1600, 1570, 1110, 750 cm^{-1}. FABMS: *m/z* 814 $(M + 2)^+$, 813 $(M + 1)^+$ 812 $(M)^+$.

C3 Ene-Capped Porphyrin VICH$_2$. **VICH$_2$** was prepared in 4% yield as purple plates from **15** by a similar procedure used in the preparation of **VIAH$_2$**. Mp >300 °C. $R_f = 0.43$ (25% ethyl acetate/hexanes), 0.35 (9% diethyl ether/dichloromethane). ^{1}H NMR:[36b] see Table II. IR: 3300 (N–H), 2920, 2850, 1460, 1350, 1180, 1110, 970, 800, 730 cm^{-1}. FABMS: *m/z* 1003 $(M + 1)^+$, 1002 $(M)^+$. UV/vis (log ε): 371.0 (4.32), 423.0 (5.58), 488.5 (3.51), 518.0 (4.21), 553.0 (3.74), 594.5 (3.65), 651.0 (3.49) nm.

(C4 capped porphyrinato)iron(III) Chloride (17). To a mixture of **VIAH$_2$** (freshly purified, 21.00 mg, 0.0198 mmol) and ferrous chloride tetrahydrate (commercial, 24 mg, 0.14 mmol) was added dry chlorobenzene (10 mL) under argon. The solution was degassed by 3 freeze–pump–thaw cycles and the mixture was refluxed. The reaction was followed by TLC and by measurement of the electronic absorption spectra of aliquots of the solution. After 3 h, the insertion was complete and the solvent was evaporated. The residue was dissolved in chloroform (40 mL) and washed with hydrochloric acid (10 mL of 0.1 N solution). After the solution was dried over anhydrous sodium sulfate the solvent evaporated, column chromatography on silica gel (5 g, eluted with 5% methanol/dichloromethane) gave the pure product **17** in quantitative yield (22.8 mg). $R_f = 0.33$ (5% methanol/dichloromethane). ^{1}H NMR (relaxation delay 50 ms; spectral width ±62500 Hz): δ 80.8 (br, β-H), 14.5 (s, 4″-H), 13.7 (s, 6″-H), 13.5 (s, 5″-H), 12.1 (s, 3″-H), −1.2, −1.9, −3.5 ppm. IR: 2900, 1040 cm^{-1}. FABMS: Calcd for $C_{72}H_{74}ClFeN_4O_4$: 1149.5. Found: *m/z* 1149.7 $(M)^+$, 1114.2 $(M - Cl)^+$. UV/vis (log ε): 374.5 (4.58), 417.5 (4.89), 508.5 (3.99), 576 (3.59), 655 (3.31), 692 (3.25) nm.

(C4 capped porphyrinato)iron(III) Hexafluoroantimonate (18). To a solution of **17** (22.8 mg, 0.019 mmol) in dry toluene (15 mL) was added solid silver antimonate (10.4 mg, 0.03 mmol) and then the whole mixture was refluxed for 3 h, at which time the visible absorption bands of **17** had disappeared. The solvent was removed and the residue was filtered through silica gel column (eluted with 5% methanol/dichloromethane), providing 25.0 mg of **18** as purple crystals (98%). $R_f = 0.40$ (5% methanol/dichloromethane). ^{1}H NMR (relaxation delay 50 ms; spectral width ±71428 Hz): δ 79.9 (br, β-H), 13.7 (br composite peaks), 7.8, 7.6 (aromatic protons), −0.5, −1.9, −3.5 ppm. FABMS: *m/z* 1114.5 $(M - SbF_6)^+$. UV/vis (log ε) (toluene): 415.5 (4.94), 571.5 (3.78), 611 (3.40), 682 (2.85) nm. UV/vis (log ε) ($CHCl_3$): 416 (4.97), 507 (3.97), 576 (3.52), 650 (3.35) nm.

Equilibrium Study. Toluene was dried over calcium hydride and then distilled. *N*-Methylimidazole (MeIm, Aldrich) was distilled before use. A Cary-14 spectrometer was used for spectral measurement from 480 to 650 nm. The spectrum was recorded at 25 °C with a 1-cm path length cell. The equilibrium constant was determined from changes in the visible spectrum caused by varying the MeIm concentration in solution with a prepared initial concentration of 1.00×10^{-4} M **18** in toluene.

Acknowledgment. This work was supported by financial assistance from the National Institutes of Health and Protos Corp. of Emeryville, CA. High resolution fast atom bombardment mass spectral determinations were performed by the Midwest Center for Mass Spectrometry, a National Science Foundation Regional Instrumentation Facility (Grant No. CHE 862017.7).

Supplementary Material Available: ^{1}H–^{1}H and ^{1}H–^{13}C 2D NMR spectra of **6**, **12**, and **15**, ^{1}H 1D, ^{13}C 1D, and ^{1}H–^{1}H 2D NMR and UV/vis spectra of **VIAH$_2$**, **VIBH$_2$**, and **VICH$_2$**, UV/vis spectra of **17** and **18**, visible spectral changes for the addition of *N*-methylimidazole to a solution of **18** in toluene, a figure showing the sizes of the cavities, and stereoviews of some representative conformers as well as a table of coordinates (.CRD) file and a listing of distances and angles of the most stable conformer (31 pages). Ordering information is given on any current masthead page.

Use of Intermolecular Hydrogen Bonding for the Induction of Liquid Crystallinity in the Side Chain of Polysiloxanes

Uday Kumar, Takashi Kato,[†] and Jean M. J. Fréchet*

Contribution from the Department of Chemistry, Baker Laboratory, Cornell University, Ithaca, New York 18453-1301. *Received February 26, 1992*

Abstract: A new type of liquid crystalline side chain polysiloxane has been built through self-assembly via intermolecular hydrogen bonding between H-bond donor and acceptor moieties. Poly(methylsiloxanes) and poly(methyl-*co*-dimethylsiloxanes) with side chains containing 4-alkoxybenzoic acid pendant groups attached through aliphatic spacers were synthesized for use as H-bond donor polymers. *trans*-4-[(4-Methoxybenzoyl)oxy]-4′-stilbazole and *trans*-4-ethoxy-4′-stilbazole were prepared as representative mesogenic or nonmesogenic H-bond acceptors, respectively. Formation of the liquid crystalline polymeric complexes occurs by self-assembly of the carboxylic acid group of the polysiloxanes with the stilbazoles through H-bonding as confirmed by spectroscopic techniques. New and extended mesogens result from self-assembly and formation of a single H-bond between the carboxylic acid side chain and the pyridyl group of the stilbazoles. Formation of a side-chain liquid crystalline polymer complex does not require that either or both of the H-bonded fragments display liquid crystallinity. The phase diagrams of a variety of mixtures of the polysiloxanes and the stilbazoles have been established using synchrotron X-ray data, differential scanning calorimetry, and optical microscopy. They show complete miscibility and unusually high thermal stability of the liquid crystals over the whole composition range. X-ray diffraction studies on unoriented samples point to smectic C or smectic A phases for the various complexes. X-ray, DSC, and optical microscopy also show that several of the starting polysiloxanes themselves have smectic C phases with their alkyl chains in an extended conformation. This liquid crystallinity results from dimerization of the benzoic acid moieties.

Introduction

Liquid crystalline polymers have great potential for various functional and high-performance materials.[1,2] For conventional side-chain liquid crystalline polymers, mesogenic units based on homologs of low molecular weight liquid crystals are attached to the polymer backbones as pendant groups through flexible aliphatic spacers using covalent bonding.[3-5] Polymethacrylates, polyacrylates, and polysiloxanes are generally used as the backbones of choice for side-chain liquid crystalline polymers. The most frequently used side-chain mesogens have cyano, nitro, or alkoxy groups as terminal units because these groups induce dipole–dipole intermolecular interactions, which contribute to the overall stability of the mesophase. When these polymers are used for electro-optic devices, the presence of such dipoles is also of great importance in aligning the mesogens in an applied electric field.

Scheme I

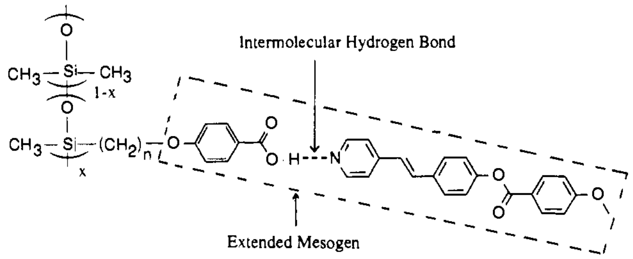

In addition to dipole–dipole interactions, various molecular interactions may widen the varieties of liquid crystalline polymers that are available. Our strategy is to utilize H-bonding as the powerful intermolecular interaction ultimately responsible for overall mesomorphicity to create a new class of side-chain liquid crystalline polymers. Hydrogen bonding is one of the key interactions for molecular aggregates in nature. However, intermolecular hydrogen bonding has, in the past, been considered deleterious for thermotropic liquid crystallinity, except for a few systems.[6-9] We have hypothesized that proper control of hydrogen bonding greatly induces the molecular ordering of thermotropic liquid crystals. Our initial approach[10] involved a 4-oxybenzoic acid moiety (capable of H-bonding interactions) that was introduced as a pendant group on a polyacrylate backbone. Subsequent complex formation between this polymer and a stilbazole moiety

---

[†] Present address: University of Tokyo, Institute of Industrial Science, Tokyo 106, Japan.

(1) Ciferri, A., Krigbaum, W. R., Meyer, R. B., Eds. *Polymer Liquid Crystals*; Academic: New York, 1982.
(2) Chapoy, L. L., Ed. *Recent Advances in Liquid Crystalline Polymers*; Elsevier: London, 1985.
(3) Ringsdorf, H.; Schneller, A. *Br. Polym. J.* **1981**, *13*, 430.
(4) Finkelmann, H.; Rehage, G. *Adv. Polym. Sci.* **1984**, *60/61*, 99.
(5) Shibaev, V. P.; Plate, N. A. *Adv. Polym. Sci.* **1984**, *60/61*, 173.
(6) Aharoni, S. M. *Macromolecules* **1988**, *21*, 1941.
(7) Jeffrey, G. A. *Acc. Chem. Res.* **1986**, *19*, 168.
(8) Bennett, G. M.; Jones, B. *J. Chem. Soc.* **1939**, 420.
(9) Gray, G. W.; Jones, B. *J. Chem. Soc.* **1953**, 4179.
(10) Kato, T.; Fréchet, J. M. J. *Macromolecules* **1989**, *22*, 3818; **1990**, *23*, 360.

0002-7863/92/1514-6630$03.00/0